ISSN 0016-7029, Geochemistry International, 2007, Vol. 45, No. 10, pp. 998–1011. © Pleiades Publishing, Ltd., 2007.
Original Russian Text © V.V. Murzin, S.N. Shanina, 2007, published in Geokhimiya, 2007, No. 10, pp. 1085–1099.

Fluid Regime and Origin of Gold-Bearing Rodingites from the Karabash Alpine-Type Ultrabasic Massif, Southern Ural

V. V. Murzin[a] and S. N. Shanina[b]

[a] *Zavaritskii Institute of Geology and Geochemistry, Ural Division, Russian Academy of Sciences, Pochtovyi per. 7, Yekaterinburg, 620151 Russia*
e-mail: murzin@igg.uran.ru

[b] *Institute of Geology, Komi Scientific Center, Ural Division, Russian Academy of Sciences, Pervomaiskaya ul. 54, Syktyvkar, 167982 Komi Republic, Russia*
e-mail: Shanina@geo.komisc.ru

Received April 14, 2006

Abstract—The rodingites of the Karabash Massif are distinguished by the presence of native cupriferous gold. This zonal hydrothermal–metasomatic complex was formed in three stages. The inner zone of rodingite proper is made up of chlorite–andradite–diopside rocks of stage 1, which are cut by diopside veinlets of stage 2 and calcite veinlets of stage 3. The intermediate zone consists of chloritolites, which give way to the antigorite and chrysotile–lizardite serpentinites of the outer zone. Thermometric and cryometric studies and gas chromatography showed that the gold-bearing rodingites of stages 1 and 2 were formed at t = 420–470°C, P = 2–3 kbar, and X_{CO_2} = 0.001–0.02, i.e., under conditions typical of rodingite formation. The final stage was accompanied by a decrease in P–T parameters (0.5–1.0 kbar and 230–310°C) and an increase in X_{CO_2} up to 0.04. The rodingite-forming fluid was extremely rich in water (X_{H_2O} = 0.942–0.981) and contained hydrogen as the major gas component (X_{H_2} = 0.012–0.023); its composition was essentially chloride–magnesium with minor amounts of $CaCl_2$ and $FeCl_2$ and a low salinity of 2.6–8.0 wt % NaCl equiv. The rodingite minerals showed the following isotopic characteristics (‰): $\delta^{18}O$ from 5.5 to 6.6 and δD from 42.8 to –44.3 for chlorite, $\delta^{18}0$ from 2.0 to 3.8 for andradite, $\delta^{18}O$ from 6.0 to 6.6 for diopside, and $\delta^{18}O$ from 10.6 to 11.4 and $\delta^{13}C$ from 0.1 to –1.8 for calcite. The chloritolite is characterized by $\delta^{18}O$ from 5.9 to 6.6 and δD from –49.8 to –64.4; the antigorite serpentinite shows $\delta^{18}O = 6.5$ and $\delta D = -65.2$; and the antigoritized chrysotile–lizardite serpentinite shows $\delta^{18}O$ from 6.8 to 6.9 and δD from –127 to –128. The calculated isotopic composition of fluid in equilibrium with various rocks suggested its metamorphic origin. It was formed from the water released during dehydration of oceanic serpentinites, from the components of ultrabasic and basic magmatic rocks, and, at the final stage, from marine carbon.

DOI: 10.1134/S0016702907100047

INTRODUCTION

Rodingites consist of pyroxene, garnet, vesuvianite, zoisite, chlorite, calcite, xonotlite, and other minerals. They are widespread in ultrabasic massifs, where they usually develop as alteration products of intermediate and basic rocks of dikes and xenoliths. More rarely, they are confined to tectonically weakened zones in ultrabasic rocks or their contacts with siliceous terrigenous rocks.

Most rodingites worldwide are barren rocks, but high contents of noble metals, primarily, gold, were occasionally observed in them. The best known gold-bearing rodingites are the rocks of the Karabash Alpine-type ultrabasic massif in the Southern Ural, which were mined at the Zolotaya Gora deposit in 1902–1946. It was shown that only serpentinites could serve as protoliths for the rodingites of this deposit, and their aposerpentinite origin was proposed [1]. Based on the high gold content and the chlorite–garnet–pyroxene composition of these rocks, a gold-bearing chlograpite (rodingite) association was distinguished [2].

The formation of ore mineralization in the gold–chlograpite (rodingite) association was initially considered as a single-stage process related to fluids supplied along deep nearly N–S-trending fault zones. According to these concepts, the rodingites were produced by the metasomatic alteration of ultrabasic rocks coeval with antigorite serpentinization. The metasomatism was accompanied by gold accumulation, which resulted in the formation of economic concentrations in the fault zones [2] only.

However, the distinguishing of the gold–rodingite association was recently disputed by Spiridonov and Pletnev [3], who studied the rocks and ores of the Karabash Massif and argued that gold mineralization in the rodingites was related to superimposed listwaenitization, and the rodingites were developed after completely reworked gabbro dikes.

In order to solve these problems, we studied the evolution of fluid regime during the formation of the rodingites of the Karabash Massif and their origin.

METHODS

Our study included measurements of the temperatures of phase transitions on heating and cooling of individual gas–liquid inclusions, determination of the gas composition of mineral-forming media entrapped in minerals, and analysis of C, O, and H isotopic compositions of rodingite minerals and country rocks. The isotopic characteristics of rodingite-forming and antigorizing fluids were calculated on the basis of fluid–mineral isotope exchange reactions. The calculations were carried out using a computer program designed by G. Beaudoin (Laval University, Canada) available on the web at http://www.ggl.ulaval.ca/personnel/beaudoin/GeorgesBeaudoin.html.

Fluid inclusions were investigated on a THMSG-600 thermostage (Linkam, England), which allows measurement of phase transitions within the temperature range from –196 to 600°C. The salt composition of solutions was determined from eutectic temperatures [4]. Salt contents in the inclusions were estimated on the basis of ice melting temperatures for the NaCl–H_20 salt system [5].

Gas compositions were analyzed by the pyrolysis method on a Tsvet-800 gas chromatograph with helium as a carrier gas, which allowed the determination of H_2, N_2, CO, CO_2, H_2O, H_2S, SO_2, CH_4, C_2H_4, C_2H_2, C_2H_6, $C_3H_6 + C_3H_8$, *iso*-C_4H_{10}, C_4H_8, and *n*-C_4H_{10}. Aliquots of 0.25–0.5-mm size fractions were preliminarily treated in heated diluted HNO_3 (1 : 1), rinsed with water, decanted, and dried at 100°C for 5–6 h. Carbonate mineral samples were not treated with acid. The temperature ranges of analysis, up to 300 and 300–600°C (300–450°C for carbonates), and the inert medium were chosen to avoid gas release at the expense of mineral decomposition, as well as chemical interaction between gases. The upper temperature limit is more than 200°C higher than the homogenization temperature of inclusions, which provided their essentially complete decrepitation. The dynamics of gas release was additionally evaluated by the stepped heating of some samples up to 800°C, i.e., above the temperature of the beginning of the breakdown of rock-forming minerals.

The isotopic composition of minerals was determined at the Analytical Center of the Far East Geological Institute, Far East Division, Russian Academy of Sciences on a Finnigan MAT 252 double-inlet mass spectrometer. Sample preparation for mass spectrometric investigations included fluorination for the oxygen isotope analysis of silicates, laser technique of water extraction for hydrogen isotope analysis [6], and a treatment with 100% phosphoric acid for oxygen and carbon isotope measurements in carbonates [7]. The reproducibility of $\delta^{18}O$, $\delta^{13}C$, and δD determination was 0.1, 0.05, and 2.5‰, respectively (1σ).

GEOLOGICAL SETTING AND FORMATION STAGES OF THE GOLD-BEARING RODINGITES

The Karabash Alpine-type ultrabasic massif is located in the southern Urals in the Main Ural Fault Zone, which separates the paleocontinental and paleooceanic segments of the Urals. The massif is part of a serpentinite diapir, which is confined to the central portion of the fault zone and represents the extruded melanocratic basement ($O_{2–3}$) of the Silurian–Devonian volcanosedimentary complexes of the Magnitogorsk megasynclinorium. The volcanic and sedimentary rocks are strongly deformed into a series of slices divided by east-dipping reverse faults. A series of steep reverse faults was formed in the core of the diapir during its extrusion owing to latitudinal compression (after D_3). In the present-day structure, they are marked by schistose serpentinites and serpentine melange with fragments of volcanogenic and sedimentary rocks [8]. The massif is made up of predominant apoharzburgite and apodunite antigorite serpentinites and minor amounts of chrysotile and lizardite serpentinites. Scarce thin bodies of clinopyroxenite and other rocks were documented [3].

Rodingites form an almost uninterrupted 3-km-long band of submeridional orientation in the central part of the massif. Small magnetite–chlorite–carbonate, magnetite–chlorite, garnet–chlorite, and quartz–riebeckite bodies form chains in the marginal parts of the massif. Tourmaline-bearing quartz–fuchsite–carbonate listwaenites after ultrabasic rocks were found at the southern contact of the massif with the volcanosedimentary sequence.

The rodingite bodies are composed of variable amounts of diopside, garnet, and chlorite of varying grain sizes. They are rimmed by the zones of chloritolites, which grade into chrysotile or antigorite serpentinites. The massive rodingites and chloritolites are cut by a network of ladder veins of essentially diopside or calcite compositions. The rodingite bodies are up to 3 m thick and contain gold over the entire length of the band. However, economic gold concentrations were found only within an area 350–400 m long in the central part of the band.

The Zolotaya Gora deposit has been described in a number of publications, including monographs [3, 9]. The most comprehensive data on the composition and crystallization order of rodingite minerals in various rock types were reported by Spiridonov and Pletnev [3]. These authors distinguished early rodingites, late

rodingites, chloritolites of reaction rims, and three generations of late rodingite veins. All the rocks were considered as barren products of regional pre-Carboniferous low-grade metamorphism of Ti-gabbro dikes ($D_{2–3}$).These authors argued that the gold concentration was related to superimposed listwaenitization, which was manifested by calcite veinlets with low-grade sulfide and native metal mineralization, including cupriferous gold. The listwaenites are genetically related to the derivatives of the Early Carboniferous granodiorite association consisting of unaltered quartz diorites, plagiogranites, and plagiogranite porphyries, which were found by Spiridonov as small bodies at the Zolotaya Gora deposit.

The distinguishing of the beresite–listwaenite metasomatic association in that deposit was repeatedly criticized by Uralian geologists (R.O. Berzon and V.N. Sazonov). We also agree with this criticism. This concept is in conflict with some facts, including the absence of the quartz + fuchsite + carbonate (magnesite–breinerite, dolomite, and calcite) assemblage, which is typical of listwaenite, and the relatively high precipitation temperature of gold, which is represented by exsolved gold–silver–copper solid solutions (more than 400°C) [10–12]. In addition, our observations and the available published and unpublished materials obtained during the mining of the deposit (M.P. Lozhechkin, A.P. Perelyaev, N.I. Borodaevskii, and others) indicate a spatial and genetic relation between the gold mineralization and rodingites. This is supported by the fact that gold was found, not only in carbonate-bearing units, but in all the members of the multistage zonal hydrothermal–metasomatic rodingite column. Moreover, according to our observations, carbonate is most abundant in the northern part of the rodingite zone, whereas the Zolotaya Gora deposit is situated in its central part. The ambiguous interpretation of carbonate as a host for cupriferous gold is presumably caused by the poor knowledge of this problem and biased sampling of gold-bearing rocks in mine waste-rock dumps.

These data indicate that the sequence of mineral formation proposed by Spiridonov can be significantly simplified. The approach used by us is accepted in ore geology and is based on the recognizing of significant duration of particular mineralization episodes, as a basis for the distinguishing of phases, and the existence of periods of deformations within phases separating stages with different mineral assemblages. Based on this approach to the interpretation of the results of comprehensive mineralogical investigations [3], we conclude that ore mineralization developed within a single phase during rodingite formation and included three stages.

The rodingites of stage 1 are dark-colored fine- to medium-grained chlorite, garnet–chlorite, and vesuvianite–garnet–chlorite rocks (early rodingites after Spiridonov), which are gradually replaced by chlorite–garnet–pyroxene rocks with variable mineral proportions and different colors (late rodingites after Spiridonov). Within a 3-m-thick zone, the enclosing serpentnites were simultaneously replaced by chloritolites, which are composed of almost monomineralic fine-grained chlorite with serpentinite relics and disseminated magnetite replacing Cr-spinel. The fine-grained rodingites of stage 1 contain particles of chalcocite and cupriferous gold, which consists of tetraauricupride (AuCu) rimmed by auricupride (Cu_3Au).

The rodingites of stage 2 are separated from the early rodingites by intramineral deformations, which produced sublatitudinal south-dipping fractures. Along these fractures, the rodingites were recrystallzied to form ladder veinlets of coarse-grained rodingites of stage 2 (the latest rodingites of the first and second generations according to Spiridonov). The rocks of stage 2 are dominated by low-Fe or Fe-free diopside with less abundant chlorite, hydroandradite, magnetite, and ilmenite. The diopside veinlets contain the largest particles of cupriferous gold (up to 2–3 mm) consisting of auricupride (Cu_3Au) and Hg-bearing electrum.

The recrystallization was locally followed by the redeposition of material and its transportation over a distance of 2 m into the enclosing serpentinites, where 10-cm-thick diopside veins were formed. The serpentinites and chloritolites adjacent to the rodingites were again chloritized along a network of thin fractures. Compared with the early chlorite, the late chlorite is coarser grained and often contains cupriferous gold, which forms exsolution products of gold–silver–copper solid solutions with a gold content of more than 50 at % [12]. Chlorite, diopside, and diopside–chlorite veinlets rim the chlograpite bodies, with the maximum thickness up to 1.5 m in the hanging wall.

The formation of ore mineralization was completed by calcite deposition (stage 3) in the rodingites and, locally, in the chloritolites and serpentinites (the latest rodingites of the third generation by Spiridonov). Calcite deposition postdated the local deformation and recrystallization of the early rodingites. Calcite forms thin (up to 2–3 cm) veinlets and occurs in the mineral aggregates of coarse-grained rodingites. Magnetite, titanite, native copper, and, according to [3], cupriferous gold were deposited during stage 3. Calcite–chlorite rocks with relict serpentine were developed in the pinches of rodingite bodies and in the adjacent serpentinites.

The most complete list of ore minerals identified in the deposit was presented by Spiridonov and Pletnev [3]: magnetite, ilmenite, chalcocite, maucherite, nickeline, millerite, greenockite, breithauptite, native copper, stibium, lead, nisbite ($NiSb_2$), seinajokite ($FeSb_2$), ullmannite (NiSbS), cuprostibite (Cu_2Sb), zlatogorite ($CuNiSb_2$), gudmindite (FeSbS), galena, auricupride (Cu_3Au), cuproauride (AuCu), phase $CuAu_3$, phase Cu_2Au_3, Hg-electrum, Hg-kustelite, Hg-silver, and Hg-gold (fineness 815–853). Noteworthy is that even the highest grade ores have very low contents of ore

minerals. Only magnetite, ilmenite, and chalcocite amount up to a few percent, whereas other minerals are ascribed to mineralogical finds.

The highest contents of cupriferous gold are related to the ladder diopside veinlets, in which gold particles usually fill cleavage fractures in diopside or cement flaky chlorite groundmass and occasionally form ingrowths in garnet and magnetite. Similar relations of gold with minerals were observed in the rodingites and veinlets extending into the country rocks. Native gold was described in [3, 12, 13, etc.].

P–T CONDITIONS OF RODINGITE FORMATION

Experimental and thermodynamic modeling of rodingite formation indicates that the mineral composition of rodingites is mainly controlled by temperature and the compositions of fluid phase, primarily CO_2 content [14, 15]. Favorable conditions for rodingite formation are temperatures below 500°C, P = 2–4 kbar, and low CO_2 content ($X_{CO_2} < 0.07$). The influence of pressure on the temperature of main equilibria is insignificant. In particular, according to experimental data, the equilibrium temperature of the diopside + garnet + chlorite + quartz assemblage is 415 ± 10°C at 2 kbar and 430°C for 4 kbar. The diopside + garnet + wollastonite + vesuvianite + quartz equilibrium is attained at 470, 500, and 520°C at 2, 4, and 6 kbar, respectively.

The mineral assemblages of the rodingites of stages 1 and 2 were formed at P = 2 kbar and 420–470°C, which corresponds to temperatures estimated on the basis of phase transitions in the Au–Ag–Cu solid solutions [12]. The low-temperature limit corresponds to the stability of mineral assemblages with garnet, diopside, and vesuvianite, and the upper limit is constrained by the appearance of wollastonite above 470–500°C [14], because this mineral and products of its low-temperature decomposition (quartz and carbonate) were never observed.

The formation temperature of calcite of stage 3, which locally shows equilibrium relations with chlorite, was estimated as 230–310°C using the calcite–chlorite oxygen isotope geothermometer [16]. Lower temperature estimates (245–140°C) were obtained from the homogenization temperatures (t_{hom}) of gas–liquid inclusions in calcite [3]. Unfortunately, these values of t_{hom} cannot be considered as mineral formation temperatures (t_m), because the authors did not report the phase composition of inclusions, criteria for their identification as primary inclusions, and the type of homogenization.

We studied gas–liquid inclusions in the minerals of all of the stages of rodingite formation: calcite, diopside, chlorite, and garnet. Primary, pseudosecondary, and secondary inclusions [17] were identified. The primary inclusions are scarce and vary in size from a few micrometers to 40 μm. They have polygonal, angular-isometric, and wedge shapes and are randomly distributed in mineral grains, with the exception of diopside, where they sometimes distinctly trace growth zones. The inclusions are composed of two phases (L + G) with a gas bubble accounting for 20–30 vol %. On freezing, the bubble sharply decreases in volume and acquires angular outlines, which are smoothed at eutectic melting temperature.

The most common inclusions are pseudosecondary; they are similar to primary inclusions in shape, size, and phase composition. In the marginal parts of large diopside grains, they often have negative crystal shapes extended parallel to prism faces or healed cleavage fractures. A gas bubble occupying 5–15 vol % disappears abruptly on freezing and reappears at ice melting temperature. The secondary inclusions occur along fissures, which intersect diopside crystals in various directions. These inclusions are usually monophase (L) and less than 5 μm in size.

The primary and pseudosecondary inclusions are homogenized into a liquid phase within a wide temperature range of 115–325°C (Fig. 1). Most inclusions in the minerals of all stages are homogenized at t_{hom} = 140–220°C, which is significantly lower than our t_m estimates for the rodingites (420–470°C). The fact that t_{hom} is significantly lower than t_m can be explained by high pressures during rodingite formation. The difference between t_{hom} and t_m depends on the pressure of mineral formation and can be roughly estimated by dividing this difference by the experimentally determined "pressure correction." Since the latter is 80–90°C/kbar at t_{hom} within 150–250°C and a hydrothermal fluid salinity of 5–10% NaCl [18], the pressure of formation of stage 1 and 2 rodingites can be estimated as 2–3 kbar. The absence of evidence for fluid heterogenization during subsequent intramineral deformations and deposition of stage 3 minerals indicates that the final stage also occurred at elevated pressures. Pressures of 0.5 kbar reported in [3] for calcite formation seem to be underestimated.

The highest temperatures of t_{hom} = 250–330°C were recorded for inclusions in minerals from a diopside veinlet of stage 2, which intersects stage 1 rodingite with lower t_{hom} = 140–200°C. There are no grounds to suggest that the fluid was additionally heated during the formation of diopside veinlets (e.g., influx of a new portion of hot fluid during stage 2). Hence, the evolution of the hydrothermal system during stages 1 and 2 probably occurred at constant temperature, whereas pressure decreased from 2–3 to 1–2 kbar during interstadial deformations and subsequent deposition of diopside veinlets. The thermostatic conditions were presumably favorable for the recrystallization of material and formation of ore shoots.

SALT AND GAS COMPOSITION OF THE FLUID

The salt composition of rodingite-forming fluid was estimated from eutectic (T_{eut}) and ice melting (T_{melt})

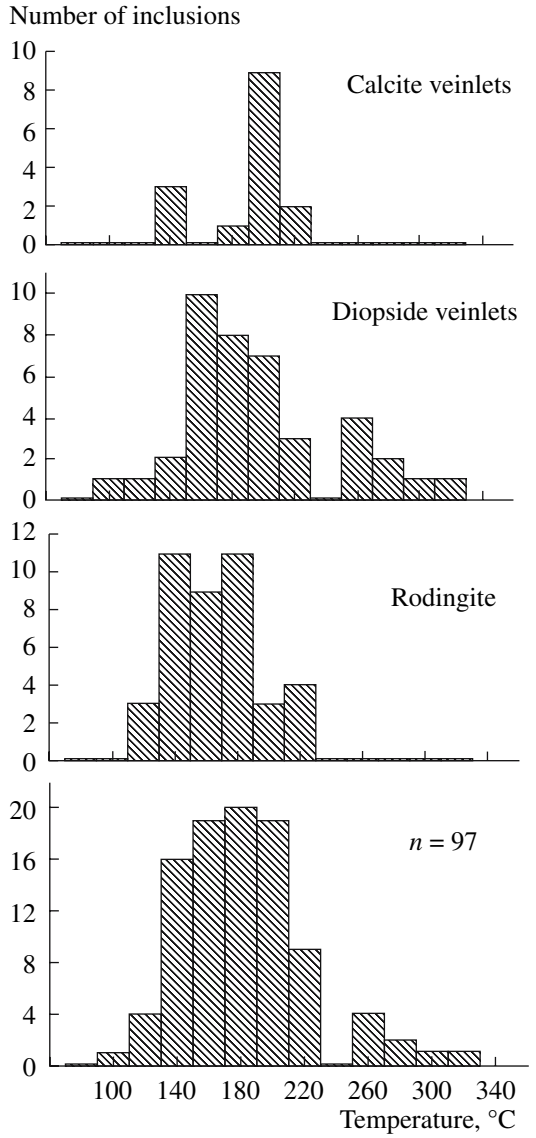

Fig. 1. Histograms of the homogenization temperatures of primary and pseudosecondary gas–liquid inclusions in rodingite minerals.

temperatures determined during freezing experiments with the largest gas–liquid inclusions in minerals. Spiridonov and Pletnev [3] reported t_{eut} from –30.6 to –36.8°C and t_{melt} from –2.3 to –5.1°C for inclusions in calcite and interpreted them as NaCl–KCl–$MgCl_2$ solutions with subordinate amounts of $CaCl_2$ and low salinity (3.9–8.0 wt % NaCl equiv.). These data were supplemented by us by temperatures for inclusions in stage 1 garnet (t_{melt} from –2.2 to –2.3°C), veinlet diopside of stage 2 in rodingite (t_{eut} from –33.3 to –34.6°C and t_{melt} from –2.2 to –2.7°C), and diopside veinlet from the country serpentinite (t_{eut} from –38 to –39°C and t_{melt} from –1.5 to –4.2°C). The obtained values of t_{eut} indicate that the rodingites were formed from a Cl–Mg fluid (t_{eut} of the pure $MgCl_2$–water system is –33.6°C). The lower t_{eut} values (from –38 to –39°C) suggest that the salt system probably contained NaCl, KCl, $FeCl_3$ or trace amounts of $FeCl_2$ and $CaCl_2$. However, only the two latter components are consistent with the observed mineral assemblages of the rodingites. The values of t_{melt} obtained for the inclusions correspond to low-salinity solutions with 2.6–6.7 wt % NaCl equiv., which were typical of all stages of rodingitization.

The chromatographic analyses of gas samples from different zones of rodingites and enclosing rocks are given in Table 1. The composition of gases accompanying rodingite formation is described by the C–O–H systems with small amounts of nitrogenous and no sulfurous gases. The fluid is sharply dominated by H_2O, CO_2, and CO; the presence of reduced gases, H_2 and CH_4, is of special importance. Heavy hydrocarbons (HHC) occur in subordinate amounts.

The step-wise heating of antigoritized chrysotile–lizardite serpentinite (10–20% antigorite) enclosing the rodingite shows a very intense gas release followed by a sharp decrease at 400–500°C; the main gas component is water (Fig. 2). Water release occurred mainly within two temperature ranges, (1) 100–300°C and (2) above 500°C, but continued up to 800°C, which was obviously related to serpentine dehydration, typically beginning at 620°C [19]. The low-temperature range of water release is presumably related to the decrepitation of gas–liquid inclusions. A sharp increase in CO_2 release at 600°C is attributed to the onset of carbonate breakdown. H_2, CH_4, and HHC were released at 500–700°C. The termination of their release at higher temperatures, when serpentine dehydration was not yet completed, indicates that the reduced gas components were not incorporated in the mineral structure but occurred in individual inclusions. The behavior of CO was peculiar. It was released with reduced gases up to 700°C, after which its release increased sharply and accompanied that of water and carbon dioxide.

The step-wise heating of a rodingite sample resulted in a significantly lower gas release compared with the serpentinite (Fig. 3). Water is the sharply predominant component of the fluid. The low-temperature range of water release at up to 200°C corresponds to the decrepitation of secondary aqueous inclusions with small amounts of CO_2, CO, N_2, and NO. Extensive release of CO_2, CO, and HHC begins above 200°C; it reaches peak values at 300–400°C and is accompanied by a decrease in water release. Even a more intense release of H_2O, CO_2, CO, H_2, and CH_4 begins above 500°C and continues up to 800°C. Similar to serpentinite, the maximum release was observed within 500–600°C for methane and 600–700°C for hydrogen. Significant part of water released at high temperature is obviously related to the dehydration of rodingite minerals (chlorite and hydrogarnet), and part of CO_2 is related to the breakdown of calcite, which occurs in the rodingite in small amounts.

In terms of gas composition, the inclusions in rodingite minerals can be divided into three types: (1) essentially

Table 1. Content of gases released during the thermal desorption of the rocks of the Zolotaya Gora deposit within 100–300 and 300–600°C

Sample No.*	t, °C	Content, μg/g sample											
		H_2	N_2	CO	CO_2	H_2O	CH_4	C_2H_4	C_2H_6	$C_3H_6 + C_3H_8$	i-C_4H_{10}	C_4H_8	n-C_4H_{10}
1283	300	n.d.	3.24	25.22	22.2	19957	0.067	0.101	n.d.	0.469	n.d.	0.061	0.263
	600	12.12	1.5	66.31	344.56	9443	23.75	3.381	0.517	2.779	0.059	0.102	0.078
1303	300	n.d.	0.67	13.04	69.87	14770	0.286	0.226	n.d.	0.815	0.121	0.225	0.703
	600	4.79	n.d.	56.91	172.2	6088	18.893	3.777	0.236	2.45	0.032	0.015	0.017
1293-3	300	n.d.	2.09	0.74	3.56	2993	0.028	0.056	n.d.	0.735	0.114	0.31	0.419
	600	10.96	n.d.	22.87	36.18	7758	3.07	2.302	0.22	5.991	0.033	0.76	0.394
1275-3	300	n.d.	2.37	1.09	4.74	1787	0.029	0.05	n.d.	n.d.	0.064	0.127	0.211
	600	9.74	n.d.	26.11	53.83	1707	1.578	1.17	0.018	2.877	0.006	0.314	0.168
1276	300	n.d.	1.54	1.56	7.56	1091	0.014	0.023	n.d.	0.199	0.004	0.264	0.462
	600	6.49	0.31	16.92	58.27	4515	3.123	1.497	0.354	2.641	0.023	0.443	0.337
1285	300	n.d.	1.56	5.02	3.01	2292	0.006	0.019	n.d.	0.209	0.002	0.138	0.246
	600	7.05	0.43	17.71	37.41	5387	6.925	3.591	1.41	8.814	n.d.	1.314	0.895
1268	300	n.d.	3.17	8.86	3.97	2434	0.015	0.022	n.d.	0.332	0.005	0.33	0.875
	600	8.8	0.62	16.68	38.34	5135	6.315	3.98	1.246	8.106	0.115	1.445	1.03
1293-2	300	n.d.	1.38	6.12	5.51	548.2	0.016	0.033	n.d.	0.218	0.004	0.306	0.347
	600	5.56	0.29	11.31	41.89	3541	2.511	1.977	0.538	2.801	0.062	0.362	0.273
1281	300	n.d.	1.75	4.92	10.28	4086	0.017	0.052	n.d.	0.412	0.007	0.358	0.612
	600	5.28	0.15	22.64	94.94	1929	9.542	4.275	1.807	7.589	0.111	1.44	1.064
1301	300	n.d.	n.d.	n.d.	7.27	273.7	0.004	n.d.	n.d.	n.d.	n.d.	n.d.	n.d.
	600	1.01	1.97	4.19	87.83	564.4	1.264	1.172	0.308	0.942	0.003	0.071	0.017

Note: *Here and in Table 2, (1) n.d. denotes below the detection limit equal to (μg/g): 1 (H_2O), 0.08 (H_2), 0.01 (N_2 and CO), 0.03 (CO_2), 1.5×10^{-5} (CH_4), 1.3×10^{-5} (C_2H_4 and C_2H_6), and 2×10^{-5} ($C_3H_6 + C_3H_8$, i-C_4H_{10}, C_4H_8, and n-C_4H_{10}). The measurement error is 16% relative. (2) 1283 and 1303, antigorite–lizardite serpentinite, southern ore body; 1293-3, chloritized serpentinite (fine-grained chloritolite), rodingite rim, northern ore body; 1275-3, medium-grained chloritolite (veinlets in fine-grained chloritolite), western ore body; 1276, veinlet of coarse-grained chlorite in chloritolite; 1285 and 1268, early chlorite–garnet–diopside rodingite; 1293-2 and 1281, late diopside rodingite; and 1301, calcite veinlet in late rodingite. Samples 1283, 1301, and 1281 are from the southern ore body; 1293 and 1301 are from the northern ore body; 1268, 1275, 1276, and 1285 are from the western ore body. Samples 1303, 1293-3, and 1293-2 showed an NO peak in the range up to 300°C.

aqueous inclusions with small amounts of CO_2, CO, N_2, and NO, which are released on heating up to 200–300°C; (2) aqueous fluids enriched in CO_2, CO, and HHC, which are released within 300–500°C; and (3) aqueous presumably gas-bearing inclusions enriched in reduced gases (H_2, CH_4, HHC), CO_2, and CO and decrepitated at temperatures >500°C. In order to analyze the evolution of the gas composition of fluid during various stages of rodingite formation, the contents of components were recalculated to mole fractions. Based on optical observations (absence of a gas bubble), the inclusions decrepitated at temperatures below 300°C are interpreted as secondary; hence, the gas released within this range reflects the composition of fluid which had lost a significant amount of gas components during mineral formation. The gas released within temperatures of 300–600°C can be used to estimate the composition of fluid during various stages of mineral formation (Table 2), because it is related to the decrepitation of mainly primary and pseudosecondary inclusions rather than the breakdown of minerals.

The initial composition of rodingite-forming fluid is characterized by the extremely high mole fraction of water, $X_{H_2O} = 0.942–0.981$, and significant predominance of hydrogen among other gas components, $X_{H_2} = 0.012–0.023$. The gases extracted from the antigoritized chrysotile serpentinite are also dominated by water; however, the serpentinizing fluid was also enriched in CO_2 and, to a lesser extent, H_2, CO, and CH_4.

As was mentioned above, mineral equilibria in the $CaO–MgO–Al_2O_3–SiO_2–CO_2–H_2O$ system are strongly dependent on CO_2 content. This parameter was calculated from gas release within 300–600°C. The results showed that the rodingites of stage 1 were formed at

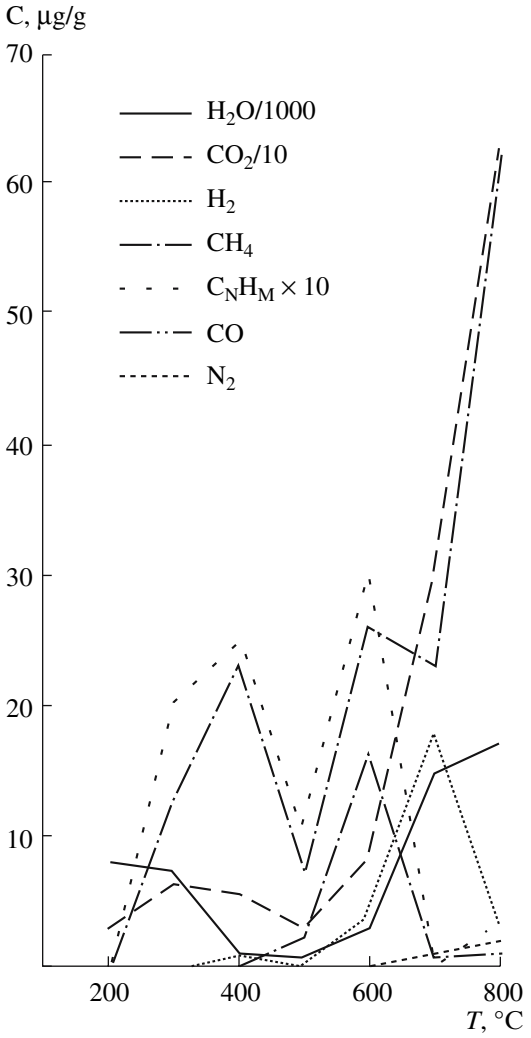

Fig. 2. Gas release from the antigorite–lizardite serpentinite (sample 3r-1303) hosting the rodingites of the deposit during step-wise heating with an increment of 100°C.

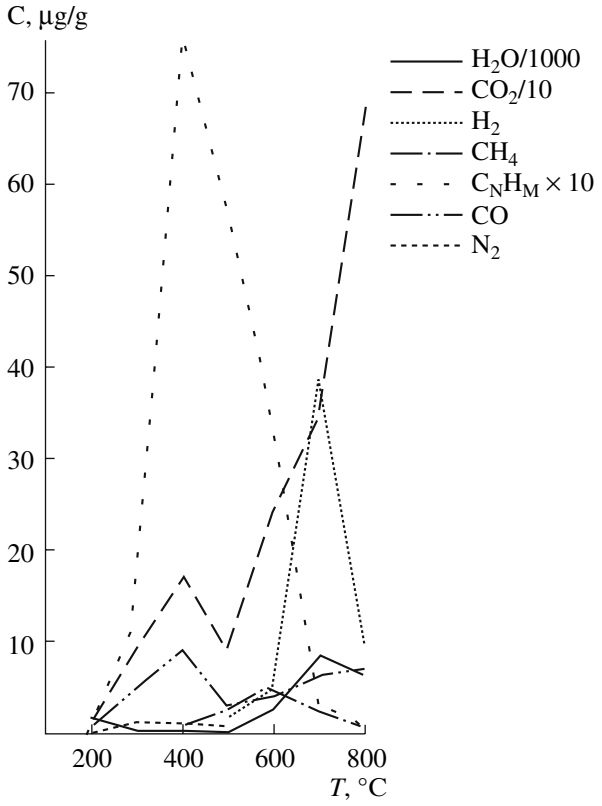

Fig. 3. Gas release from the chlorite–garnet–pyroxene rodingite (sample 3r-1285) of the deposit during step-wise heating with an increment of 100°C.

low X_{CO_2} = 0.001–0.003, which agrees with experimental data on the upper stability limit of rodingite at $X_{CO_2} = 0.007 \pm 0.001$ [14]. On the other hand, X_{CO_2} in fluid increases during the evolution of the metasomatic process up to 0.005–0.019 at stage 2 and 0.039 at stage 3.

Similar to the rodingite-forming solution of stage 1, the fine-grained chloritolites adjacent to the rodingites were formed at extremely low values of X_{CO_2} = 0.002. The coarse-grained vein aggregates of chlorite in the fine-grained chloritolite were formed at a higher CO_2 content (X_{CO_2} = 0.005–0.012) approaching that of stage 2 rodingitization. Fluid from inclusions in serpentinite also shows an increase in X_{CO_2} up to 0.011–0.014. Thus, in terms of the proportions of gas components, the fluids contributing to the formation of stage 1 and 2 rodingites and chloritolites were equilibrated and contained H_2 as the major gas component (Fig. 4). In contrast, the fluid responsible for the formation of the calcite veinlets of stage 3 and serpentinites was dominated by CO_2.

CO was found both in the rodingite-forming and serpentinizing fluids. Its mole fraction is 1.5–3.0 times lower than that of CO_2; however, these components are characterized by identical distribution in inclusions from different metasomatic zones. Similar to CO, the highest CH_4 contents (X_{CH_4} = 0.002–0.005) were found in serpentinite, late rodingite, and calcite samples. The mole fraction of nitrogen in the fluid is no higher than 0.001. It is accumulated mainly in the secondary inclusions (X_{N_2} up to 0.002), which is probably related to the fact that nitrogen is not incorporated into hydrous minerals but is accumulated in the residual fluid [20].

The redox conditions of rodingite formation were estimated from the degree of oxidation of volatiles, $CO_2/(CO_2 + CO + H_2 + CH_4)$. Based on this ratio, it was found that the rodingites and chloritolites of stages 1 and 2 were formed under reducing conditions (<0.35), whereas the calcite veinlets were formed under oxidizing conditions (0.83). The degree of oxidation of volatiles was intermediate during serpentinization.

Table 2. Composition of gases released during the thermal desorption of rocks within 300–600°C (mole fractions)

Sample No.	Rock, stage	H_2O	CO_2	CO	N_2	H_2	CH_4	ΣC_nH_m	$CO_2/(CO_2 + CO + H_2 + CH_4)$
1283	Serpentinite	0.967	0.014	0.004	0.00010	0.011	0.0027	0.0004	0.44
1303	Same	0.972	0.011	0.006	n.d.	0.007	0.0034	0.0006	0.41
1293-3	Chloritolite, I	0.983	0.002	0.002	n.d.	0.012	0.0004	0.0006	0.11
1275-3	Chloritolite, II	0.929	0.012	0.009	n.d.	0.048	0.0010	0.0015	0.17
1276	Chlorite, II	0.978	0.005	0.002	0.00004	0.013	0.0008	0.0005	0.25
1285	Rodingite, I	0.981	0.003	0.002	0.00005	0.012	0.0014	0.0014	0.16
1268	Same	0.977	0.003	0.002	0.00008	0.015	0.0014	0.0014	0.14
1293-2	Rodingite, II	0.978	0.005	0.002	0.00005	0.014	0.0008	0.0008	0.22
1281	Same	0.942	0.019	0.007	0.00005	0.023	0.0052	0.0038	0.35
1301	Calcite, III	0.935	0.039	0.004	0.00335	0.015	0.0006	0.0007	0.83

The observed systematic variations in the gas composition of fluid during various stages of rodingite formation can be explained by the influx of CO_2, CO, and CH_4 from the enclosing serpentinites during interstadial deformations and by the gradual saturation of residual fluid in CO_2 in the course of rodingitization. The enrichment of fluid in CO_2 was related to its release from serpentinite and chloritolite during the replacement of carbonate minerals by silicates and incorporation of water into the structure of hydrous minerals, primarily, chlorite. A temperature decrease up to 400°C and lower during stage 3 led to a decrease in equilibrium CO_2 contents [21], which resulted in the instability of calcium silicates and their replacement by calcite.

ISOTOPIC COMPOSITION OF MINERALS AND EQUILIBRIUM FLUID

The silicate minerals of rodingite and chloritolite of all stages show minor variations in oxygen isotopic composition. The $\delta^{18}O$ values vary from 5.5 to 6.6‰ in chlorite, from 2.0 to 3.8‰ in andradite, and from 6.0 to 6.6‰ in diopside (Table 3). In contrast, the hydrogen isotopic composition of chlorite shows wider variations. Chlorite from the rodingite shows the highest δD values from –42.8 to –44.3 ‰, and the chloritolites of stages 1 and 2 are enriched in the light hydrogen isotope, (δD from –53.3 to –55.9‰ and from –49.8 to –64.4‰, respectively). The carbon and oxygen isotopic compositions of stage 3 calcite from the rodingite and enclosing serpentinite are similar ($\delta^{13}C$ from 0.1 to −1.8 ‰ and $\delta^{18}O$ from 10.6 to 11.4‰).

Two samples of chrysotile–lizardite serpentinite (up to 10–20% antigorite) collected directly near the rodingites have $\delta^{18}O$ = 6.8–6.9‰ and δD from –127 to −128‰. The antigorite serpentinites of the Karabash Massif have a similar oxygen isotopic composition and a heavier hydrogen isotopic composition. In the northern part of the massif, rodingite boudins occur in antigorite serpentinites with $\delta^{18}O$ = 6.5‰ and δD = –65.2‰. Antigorite serpentinite at the contact with magnetite–chlorite–dolomite rocks shows $\delta^{18}O$ = 7.6‰ and δD = –89.6‰.

Considerable data have been published on stable isotope fractionation between water and minerals. This makes possible the calculation of the isotopic characteristics of equilibrium fluid within a given temperature range. Of particular importance for our study are data on isotope fractionation in systems including chlorite group minerals (clinochlore) and serpentine. The examination of the available data on the partitioning of oxygen isotopes between water and these minerals at

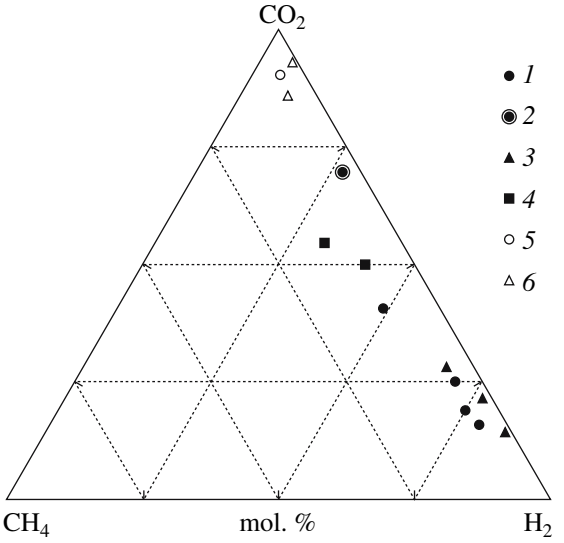

Fig. 4. Proportions of gas components during the formation of (*1–4*) the rodingites of the Zolotaya Gora deposit and (*5, 6*) some hydrocarbonic metasomatic rocks from the marginal part of the Karabash Massif: (*1*) rodingite of stages 1 and 2, (*2*) rodingite of stage 3, (*3*) chloritolite, (*4*) serpentinite, (*5*) quartz–fuchsite–carbonate listwaenite, and (*6*) magnetite–chlorite–dolomite metasomatic rock.

Table 3. Isotopic compositions of minerals from the serpentinites, rodingites, and chloritolites of the Karabash Massif

Sample No.	Rock	Mineral*, stage	$\delta^{13}C$, ‰ PDB	$\delta^{18}O$, ‰ SMOW	δD, ‰ SMOW
1303	Serpentinite hosting rodingite (inner part of the massif)	*Liz* > *chr* > *ant*	–	6.9	–127.7
1283	Same	*Liz* > *chr* > *ant*	–	6.8	–128
1380	″	*Ant*	–	6.5	–65.2
1420	Serpentinite from the western outer part of the massif	*Ant*	–	7.6	–89.6
1275	Fine-grained massive chloritolite at the contact with rodingite	*Chl*,1	–	6.4	–55.9
1293	Same	*Chl*,1	–	6.6	–53.3
1275	Chlorite veinlets in fine-grained massive chloritolite	*Chl*, II	–	6.2	-49.8
1276	Same	*Chl*, II	–	6.1	–
1277	″	*Chl*, II	–	5.9	–64.4
1293	″	*Chl*, II	–	6.3	–
1268	Variably grained early rodingite	*Chl*, I	–	6.1	–44.3
		Di, I	–	6.3	–
		Ad, I	–	2.0	–
1279	Same	*Chl*, I	–	6.5	–42.8
		Di, I	–	6.6	–
		Ad, I	–	3.5	–
1285	″	*Chl*, I	–	6.1	–43.6
		Di, I	–	6.0	–
		Ad, I	–	3.6	–
1299	Late rodingite (pockets and veinlets)	*Di*, II	–	6.2	–
1270	Same	*Ad*, II	–	3.8	–
		Di, II	–	6.2	–
1275	″	*Di*, II	–	6.5	–
1301	″	*Di*, II	–	6.3	–
1296	Same, with calcite	*Di*, II	–	6.1	–
		Cal, III	0.1	11.2	–
1297	″	*Cal*, III	–1.2	11.4	–
1300	Calcite–chlorite rock with relics of serpentine at the contact with rodingite	*Chl*, III	–	5.5	–62.8
		Cal, III	–0.9	11.2	–
1301	Same	*Chl*, III	–	5.7	–
		Cal, III	–1.8	10.6	–

* Mineral abbreviations: *Liz*, lizardite; *Chr,* chrysotile; *Ant*, antigorite; *Di*, diopside, *Ad*, andradite; *Chl*, chlorite; and *Cal*, calcite.

230–500°C showed an insignificant difference (<1.5‰) between the values of $1000\ln\alpha$ ($\Delta^{18}O_{mineral-water}$) reported by different authors [16, 22, 23]. A significantly higher discrepancy was reported only in [24] for temperatures above 400°C (up to 2.5° at 500°C). At 300°C, there is almost no oxygen isotope fractionation, and minerals and water have identical isotopic compositions. The most reliable are average data reported in [16].

The only experimental study on hydrogen isotope partitioning between chlorite and water [25] indicates a relatively small isotope fractionation effect at 500–700°C: $1000\ln\alpha$ varies from –30.2 to –27.9‰. The interpolation of these data to 400°C yields $1000\ln\alpha$ = –32.3‰. These values are consistent with the results for natural samples [26]: $1000\ln\alpha$ varies from –45 at 300°C to –35° at 500°C. The available data on hydro-

Table 4. Calculation of possible ranges of the isotopic composition of water and CO_2 of fluid for various stages of rodingite formation

Rock, stage	Mineral	Isotopic composition of minerals, ‰ (number of analyses)			Calculated isotopic composition of fluid, ‰*			
		$\delta^{18}O$	δD	$\delta^{13}C$	$\delta^{18}O$ (H_2O)	$\delta^{18}O$ (CO_2)	δD (H_2O)	$\delta^{13}C$ (CO_2)
Early rodingite, 1	Chlorite	6.1…6.5(3)	–42.8…–44.3(3)	–	7.2…7.8	–	–3.6…–13.4	–
	Andradite	2.0…3.6(3)	–	–	5.6…5.9	–	–	–
	Diopside	6.0…6.6(3)	–	–	7.8…8.3	–	–	–
Chloritolite, 1	Chlorite	6.4…6.6 (2)	–53.3…–55.9 (2)	–	6.5…7.9	–	–14.6…–24.4	–
Late rodingite, 2	Andradite	3.8(1)	–	–	6.3…6.7	–	–	–
	Diopside	6.1…6.5 (5)	–	–	7.8…8.3	–	–	–
Chloritolite, 2	Chlorite	5.9…6.3 (4)	–49.8…–64.4 (2)	–	7.1…7.7	–	–9.8…–34.2	–
Calcite veinlets and chlorite–calcite rocks, 3	Calcite	10.6… 11.4(4)	–	0.1…–1.8 (4)	2.3…5.9	19.9…21.3	–	–0.9…2.2
	Chlorite	5.5…5.7 (2)	–62.8 (1)	–	3.7…5.7	–	–17…–18	–

* The oxygen isotopic composition of fluid was calculated for temperatures of 400–500°C (stages 1 and 2) and 230–310°C (stage 3) using the following equilibria: andradite–water, diopside–water [32], clinochlore–water [16], and calcite–water [33]; the hydrogen isotopic composition was calculated from the chlorite–water equilibrium [25, 26]; and the carbon and oxygen isotopic compositions of CO_2 of fluid was calculated from the calcite–CO_2 equilibrium [33, 34].

gen isotope fractionation between water and serpentinite are much less consistent. The most extensive experimental data for a wide temperature range were reported in [27]. However, they show a significant discrepancy with empirical observations on natural samples [20] at temperatures below 400°C. On the other hand, the natural data agree with some experiments at 400 [29], 200, and 100°C [30, 31]. The value of $1000\ln\alpha$ is strongly pressure-dependent (0.001 per 2.5 kbar) in the low-temperature region (lizardite–water equilibrium). The difference between $1000\ln\alpha$ values reported by different authors is less significant at temperatures of 400°C and higher, which correspond to the formation conditions of rodingites and antigorite serpentinites. This allowed us to estimate the range of water isotopic composition in equilibrium with antigorite. The value of $1000\ln\alpha$ is –20‰ [29] or –13‰ [27] at 400°C, and the differences diminish at 500°C.

Given these data, the isotopic composition of rodingite-forming fluid can be calculated (Table 4). Fluid in equilibrium with antigorite serpentinite adjacent to the rodingite at 400–500°C was characterized by $\delta^{18}O_{fl}$ from 7.4 to 8.0‰ and δD from –52 to –45‰; and that in equilibrium with the serpentinite from the marginal part of the massif showed $\delta^{18}O_{fl}$ from 8.5 to 9.1 and δD from –77 to –70‰.

ORIGIN OF RODINGITE-FORMING FLUID

There are several opinions on the origin of rodingite-forming fluid in the ultrabasic massif studied. Early researchers (E.A. Kuznetsov, A.P. Perelyaev, and N.I. Borodaevskii) believed that the rodingites were related to "granitizing" solutions. According to M.P. Lozhechkin, R.O. Berzon, V.N. Sazonov, and other geologists, the rodingites (chlograpites) are by-products of antigorite serpentinization caused by mantle fluids ascending along deep-seated faults. Spiridonov and Pletnev [3, 35] proposed a multistage model of their formation. According to this model, the early rodingites of stage 1 were produced by the pregranite low-grade regional metamorphism of gabbroid dikes under prehnite–pumpellyite and pumpellyite–actinolite facies conditions. This metamorphism affected both the ultrabasic rocks and the enclosing volcanosedimentary sequences. The late rodingites of stage 2 were formed during local low-grade metamorphism caused by an H_2O–CO_2 fluid flow accompanying the emplacement of the granodiorite association. The formation of the calcite-dominated gold-bearing rodingites of stage 3 was related to the fluids that separated during the emplacement of granitoid dikes of the same granodiorite association.

Our data are in general not consistent with the suggestion that postmagmatic fluids took part in all stages of the formation of gold-bearing rodingites. Such hydrothermal solutions usually produce talc–carbonate metasomatites or listwaenites in ultrabasic rocks. They are more enriched in CO_2 than the fluids observed in the rodingites and contain H_2S. In particular, the fluids that produced the listwaenites and gold-bearing magnetite–carbonate–chlorite metasomatites of the Karabash Massif were characterized by X_{CO_2} values of 0.137 and 0.087–0.124, respectively. The oxygen isotope composition of the rodingite-forming fluid shows magmatic and juvenile signatures (Fig. 5). However, the same isotopic composition is characteristic of metamorphic water released from the metamorphic rocks that were not involved into the sedimentary cycle, i.e., having low

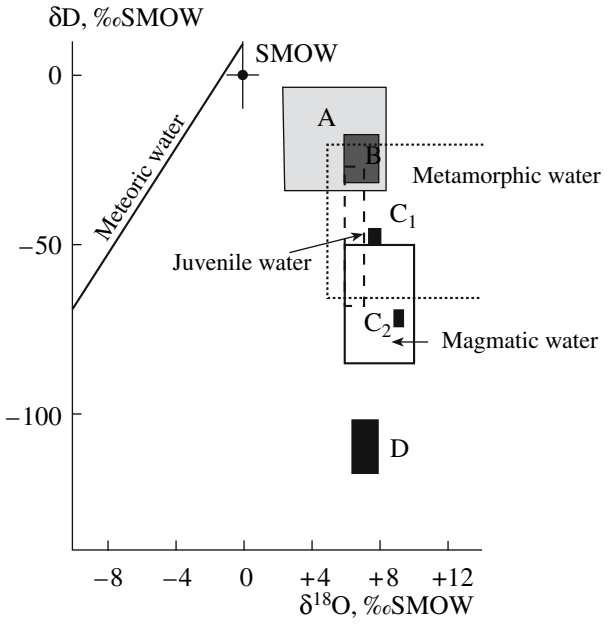

Fig. 5. Isotopic composition of fluid during the formation of rodingite (field A), chloritolite (field B), antigorite serpentinite hosting rodingite (field C_1), antigorite serpentinite from the marginal part of the massif (field C_2), and antirogite–chrysotile serpentinite (field D). Also shown are the fields of water reservoirs participating in hydrothermal ore formation (these compositions are based on the analysis of the available published data of H.P. Taylor Jr., I. Friedman, G. Faure, J. Hoefs, and others).

$\delta^{18}O$ values [36]. The hydrogen isotopic composition of rodingite-forming fluid (δD_{H_2O} from –4 to –34‰) does not overlap that of magmatic fluids and falls between the fields of metamorphic and marine waters.

The obtained isotopic data indicate the participation of marine carbonates in rodingite formation. The isotopic composition of carbon of CO_2 from stage 3 fluid showed higher $\delta^{13}C_{CO_2\,(fl)}$ values (from –0.9 to +2.2‰) than juvenile or magmatic fluids. Its composition fits the carbon isotopic composition of marine carbonates (from 0 to +5‰) [36] and was probably slightly depleted in ^{13}C owing to mixing with isotopically light serpentinite components (CO_2, CO, and CH_4). The $\delta^{18}O_{CO_2\,(fl)}$ values of this CO_2 in equilibrium with calcite were estimated as 19–21.3‰, which could be expected for CO_2 released during the dissolution of marine carbonate from metamorphosed oceanic serpentinites or its replacement by silicates.

It seems evident, that the fluid released during the regional metamorphism of the ophiolite complex could hardly participate in the formation of the Zolotaya Gora rodingites. Fluids generated during the regional metamorphism of the volcanosedimentary framing of the ultrabasic rocks must be strongly enriched in CO_2 ($X_{CO_2} > 0.1$) and nitrogen. It was shown [20] that the regional metamorphism of ophiolite slices together with the enclosing volcanosedimentary sequences produced an H_2O–CO_2 fluid with minor amounts of other components (CO, N_2, CH_4, and H_2). Its gas composition depends on the proportions of the magmatic and sedimentary constituents of the ophiolite complex and the degree of its deformation. The X_{CO_2} values calculated using the data of [20] suggest that the fluid released during the metamorphism of volcanosedimentary rocks was characterized by X_{CO_2} = 0.12–0.47, the fluid released from metamorphosed intermediate and mafic lavas had X_{CO_2} = 0.03–0.21 (at X_{N_2} up to 0.56), and that generated in gabbro showed X_{CO_2} from 0.03–0.08 to 0.2. A characteristic gaseous component of the fluid is nitrogen, the content of which depends on the composition of initial rocks and decreases in the sequence intermediate and basic lavas (up to 163 mg/kg), gabbro (up to 47 mg/kg), and volcanosedimentary rocks (up to 5 mg/kg).

Thus, the rodingite-forming fluid is in essence metamorphic but shows some specific features. On the one hand, it was probably released during the local metamorphism that altered the rocks of the massif but did not affect the surrounding Paleozoic volcanosedimentary rocks, and, on the other hand, its initial isotopic composition was enriched in heavy hydrogen and carbon isotopes owing to the involvement of water and CO_2 of marine origin. In addition, a distinct geochemical specialization of the rodingites for Ti, P, and Cu indicates that basic rocks, probably the gabbro and pyroxenites of the melanocratic basement, were involved in the metamorphic process.

Similar isotopic signatures were found in voikarite, antigorite and olivine–antigorite rocks from the Alpine-type ultrabasic massifs of the Polar Urals. These rocks have a uniform oxygen isotopic composition and a widely varying hydrogen isotopic composition and were formed by local prograde metamorphism. It was supposed that these rocks were formed under the influence of metamorphic fluid released during the deserpentinization of seafloor ultrabasic rocks [37]. It was also proposed that subduction-released fluid was involved in the formation of noble-metal-bearing metasomatites, including rodingites [38, 39]. In our opinion, at the current stage of knowledge, metamorphosed oceanic serpeninites at the base of an exhumed tectonic wedge can be considered as the most probable sources of rodingite-forming metamorphic fluid. Metamorphism releases both hydroxyl (deserpentinization) water and, to a lesser extent, pore seawater. Most of the determinations of ice melting temperatures in gas-liquid inclusions in minerals of all stages fall between –2.2 and –3.3°C, which corresponds to a salinity of 3.7–5.4 wt % NaCl equiv., which is only slightly higher than the salinity of the world's ocean (about 3 wt % NaCl equiv.). This model is most consistent with the obtained

data and explains the influence of marine components on the transformation of ultrabasic rocks under crustal conditions, when the direct involvement of marine components in the rodingite-forming fluid seems to be highly improbable.

The relation between rodingitization and serpentinization remains poorly understood. Many researchers suggested that the formation of rodingites was related to the "antigoritizing fluid" or, more often, that the rodingitization and serpentinization were simultaneous processes and the rodingites were by-products of serpentinization [2, 3, 11, 40–43]. These suggestions were based on the confinement of rodingite bodies to serpentinized rocks and the identical degrees of retrograde metamorphism in the rodingites and their host ophiolites. In the case of an aluminosilicate protolith, the chemistry of rodingitization is consistent with the mechanism of allochemical metamorphism. However, there are some deviations from these relationships. For instance, the high-temperature garnet- and pyroxene-bearing rodingites of the Sayan–Baikal mountain area occur in low-grade lizardite and chrysotile–lizardite serpentinites, whereas the lower grade rodingites made up of clinozoisite, epidote, amphibole, albite, chlorite, and other minerals are enclosed in antigorite serpentinites [39]. According to the model of the formation of rodingite-forming fluid through the deserpentinization of ultrabasic rocks, the zone of fluid discharge at higher levels should probably be controlled by permeability regardless of rock composition and the degree of serpentinization of ultrabasic material. In such a case, the rodingites will have a hydrothermal–metasomatic genesis.

The rodingite bodies of the Karabash Massif are hosted by serpentinites of different composition: variably antigoritized lizardite and chrysotile–lizardite or antigorite rocks. The lizardite and chrysotile serpentinites were formed at lower *P–T* parameters compared with the antigorite serpentinites and rodingites and show the lowest δD values (from –127 to –128‰). It was shown above that the gas composition of fluid inclusions in these serpentinites differs from that in the rodingites in higher mole fractions of CO_2, CO, and CH_4. The serpentinites were undoubtedly formed earlier than the rodingites and served as protoliths for the antigorite serpentinites, chloritolites, and, possibly, rodingites. The systematic changes in the hydrogen isotopic composition of fluid in equilibrium with these rocks indicate that the antigorite serpentinites could pertain to the metasomatic column (antigorite serpentinite–chloritolite–rodingite) that was produced by the interaction of the rodingite-forming metamorphic fluid (δD_{fl} from –4 to –13‰) with the early serpentinites. In such a model, the hydrogen isotopic composition of the resulting chlorite and antigorite will be controlled by the water–rock ratio (W/R) in rocks with variable permeability. Our mass balance calculations for a closed system [28] showed that the chloritolites of stage 1 (δD from –53.3 to –55.9‰) were formed at W/R = 3.5–3.7. Such high W/R values in a closed system require considerable volumes of free space, i.e., they could be attained in heavily fractured rocks. During the formation of antigorite serpentinite in the near-rodingite zone (δD = –65.2‰) and antigorite serpentinite in the marginal part of the massif (δD = –89.6‰), the W/R ratio was 1.3–2.0 and 0.5–0.7, respectively.

CONCLUSIONS

(1) The gold-bearing rodingites of the Karabash Massif are hydrothermal–metasomatic rocks, which were formed in three stages in a tectonically weakened zone with considerable volumes of free space. The interaction of the rodingite-forming fluid with serpentinites accompanied by a decrease in the water/rock ratio leads to the formation of a chloritolite zone and, possibly, antigorite serpentinites around rodingite bodies.

(2) The rodingites of stages 1 and 2 were formed under conditions typical of such rocks: t = 420–470°C, P = 2–3 kbar, and X_{CO_2} = 0.001–0.02. The final third stage was associated with a decrease in *P–T* parameters (0.5–1.0 kbar and 230–310°C) and an increase in X_{CO_2} up to 0.04. The rodingite-forming fluid was characterized by a very high water mole fraction (X_{H_2O} = 0.942–0.981), significant predominance of hydrogen among gas components (X_{H_2} = 0.012–0.023), essentially Cl–Mg composition, minor amounts of Ca and Fe chlorides, and low salinity (2.6–2.7 wt % NaCl equiv.).

(3) The rodingite-forming fluid was of metamorphic origin and involved marine water, ultrabasic and basic igneous rocks, and, during the final stage, marine carbon. This fluid was generated by the metamorphism of oceanic serpentinites and associated basic rocks. The fluid components were formed by the dehydration of rocks (deserpentinization) and, to a lesser extent, the release of seawater trapped in the pore space of serpentinites. Gold and other ore components were extracted from serpentinites and associated gabbroids.

ACKNOWLEDGMENTS

This study was financially supported by the Russian Foundation for Basic Research (project no. 04-05-64679), the Ministry of Education and Science of the Russian Federation (project no. RNP. 2.1.1.1840), and the Federal Agency on Science and Innovations (theme RI-112/001/081).

REFERENCES

1. R. O. Berzon and I. O. Fadeicheva, "Characteristics of Metasomatic Alterations at the Zolotaya Gora Gold Deposits," in *Metasomatism and Ore Formation* (UNTs AN SSSR, Sverdlovsk, 1974), pp. 63–67 [in Russian].
2. V. N. Sazonov, *Gold-Productive Metasomatic Associations of Mobile Belts (Geodynamic Settings and PTX*

Parameters of Formation: Predictive Significance (UGGGA, Yekaterinburg, 1998), [in Russian].

3. E. M. Spiridonov and P. A. Pletnev, *Zolotaya Gora Deposit of Cupriferous Gold* (Nauchnyi Mir, Moscow, 2002) [in Russian].
4. A. S. Borisenko "Cryometric Study of the Salt Composition of Gas–Liquid Inclusions in Minerals," Geol. Geofiz., No. 8, 16–27 (1997).
5. R. J. Bodnar and M. O. Vityk, "Interpretation of Microthermometric Data for H_2O–NaCl Fluid Inclusions," in *Fluid Inclusions in Minerals: Methods and Applications*, Ed. by B. De Vivo and M. L. Frezzotti (Pontignano, Siena, 1994), pp. 117–130.
6. A. V. Ignat'ev and T. A. Velivetskaya, "Laser Technique of Water Extraction from Hydrous Minerals for the Measurement of Hydrogen Isotope Composition" in *Proceedings of 17th Symposium on Isotope Geochemistry* (GEOKhI RAN, Moscow, 2004), pp. 98–99 [in Russian].
7. J. M. McCrea, "On the Isotopic Chemistry of Carbonates and Paleotemperature Scale," J. Chem. Phys. **18**, 849–857 (1950).
8. I. B. Seravkin, S. E. Znamenskii, and A. M. Kosarev, "The Main Ural Fault in the South Urals: the Structure and Main Evolution Phases," Geotektonika, No. 3, 42–64 (2003) [Geotectonics **37**, 210–231 (2003)].
9. A. P. Perelyaev, "The Zolotaya Gora Deposit," in *200th Anniversary of Gold Mining in the Urals* (UFAN SSSR, Sverdlovsk, 1948), pp. 285–295 [in Russian].
10. V. V. Murzin and V. N. Sazonov, "Origin of Cupriferous Gold Mineralization in Alpine-Type Ultramafic Rocks," Dokl. Akad. Nauk **366**, 797–798 (1999) [Dokl. Earth Sci. **366**, 634–635 (1999)].
11. V. N. Sazonov, V. V. Murzin, V. N. Ogorodnikov, and Yu. A. Volchenko, "Gold Mineralization Conjugated with Alpine-Type Ultrabasic Rocks," Litosfera, No. 4, 63–77 (2002).
12. V. V. Murzin and S. G. Sustavov, "Solid-State Transformations in Natural Cupriferous Gold," Izv. Akad. Nauk SSSR. Ser Geol., No. 11, 94–104 (1989).
13. M. I. Novgorodova, A. I. Tsepin, I. M. Kudrevich, and L. N. Vyal'sov, "New Data on the Crystal Chemistry and Properties of Natural Intermetallic Compounds of the Copper–Gold System," Zap. Vses. Mineral. O-va **106**, 540–552 (1977).
14. L. P. Plyusnina, G. G. Likhoidov, and G. P. Zaraiskii, "Physicochemical Conditions of Rodingite Formation: Experimental Data," Petrologiya **1**, 557–568 (1993).
15. G. G. Likhoidov and L. P. Plyusnina, "Rodingites of Northern Sakhalin and Physicochemical Conditions of Their Formation," Tikhookean. Geol., No. 2, 53–65 (1992).
16. Y.-F. Zheng, "Calculation of Oxygen Isotope Fractionation in Hydroxyl-Bearing Silicates," Earth Planet. Sci. Lett. **120**, 247–263 (1993).
17. E. Roedder, *Fluid Inclusions*, Rev. Mineral. **12** (1984); Mir, Moscow, 1987.
18. P. V. Klevtsov and G. G. Lemmlein, "Pressure Correction to the Homogenization Temperatures of Aqueous Solutions," Dokl. Akad. Nauk SSSR **128**, 1250–1253 (1959).
19. V. P. Ivanova, B. K. Kasatov, T. N. Krasavina, and E. L. Rozinova, *Thermal Analysis of Minerals and Rocks* (Nedra, Leningrad, 1974) [in Russian].
20. K. B. Kepezhinskas and A. A. Tomilenko, "Dynamics of Changes in Fluid Composition during the Metamorphism of Ophiolite Rocks Exemplified by the Eastern Khubsugul Area," Dokl. Akad. Nauk SSSR **285**, 963–966 (1985).
21. N. S. Nikol'skii, *Fluid Regime of Endogenous Mineral Formation* (Nauka, Moscow, 1987) [in Russian].
22. D. B. Wenner and H. P. Taylor, Jr., "Temperatures of Serpentinization of Ultramafic Rocks Based on $^{18}O/^{16}O$ Fractionation between Coexisting Serpentine and Magnetite," Contrib. Mineral. Petrol. **32**, 165–185 (1971).
23. D. R. Cole and E. M. Ripley, "Oxygen Isotope Fractionation between Chlorite and Water from 170 to 350°C: A Preliminary Assessment Based on Partial Exchange and Fluid/Rock Experiments," Geochim. Cosmochim. Acta **63**, 49–457 (1998).
24. S. M. Savin and M. Lee, "Isotopic Studies of Phyllosilicates," in *Hydrous Phyllosilicates*, Rev. Mineral. **19**, 189–223 (1988).
25. N. I. Graham, J. Atkinson, R. S. Harmon, "Hydrogen Isotope Fractionation in System Chlorite–Water," in *NERC 6th Progress Report of Research 1981–1984*, NERC Publication Series D., No. 25, 139 (1984).
26. H. P. Taylor, Jr., "The Application of Oxygen and Hydrogen Isotope Studies to Problems of Hydrothermal Alteration and Ore Deposition," Econ. Geol. **69**, 843–883 (1974).
27. H. Sakai and M. Tsutsumi, "D/H Fractionation Factors between Serpentine and Water at 100 to 500°C and 2000 bar Water Pressure, and the D/H Ratios of Natural Serpentines," Earth Planet. Sci. Lett. **40**, 231–242 (1978).
28. D. B. Wenner and H. P. Taylor, "Oxygen and Hydrogen Isotope Studies of the Serpentinization of Ultramafic Rocks in Oceanic Environments and Continental Ophiolite Complexes," Am. J. Sci. **273**, 207–239 (1973).
29. O. Suzuoki and S. Epstein, "Hydrogen Isotope Fractionation between OH-Bearing Minerals and Water," Geochim. Cosmochim. Acta. **40**, 1229–1240 (1976).
30. V. A. Grinenko, S. D. Mineev, A. L. Devirts, and E. P. Lagutina, "Hydrogen Isotope Fractionation in the Lizardite–Water System at 100°C and 1 atm," Geochem. Int. **24**, 100–104 (1987).
31. S. D. Mineev and V. A. Grinenko, "The Pressure Influence on Hydrogen Isotopes Fractionation in the Serpentine-Water System," in *Proceedings of V.M. Goldschmidt Conference, Heidelberg, Germany, 1996*, (Heidelberg, 1996), Vol. 1, p. 404.
32. Y.-F. Zheng, "Calculation of Oxygen Isotope Fractionation in Anhydrous Silicate Minerals," Geochim. Cosmochim. Acta **57**, 1079–1091 (1993).
33. Y.-F. Zheng, "Oxygen Isotope Fractionation in Carbonate and Sulfate Minerals," Geochem. J. **33**, 109–126 (1999).
34. H. Ohmoto and R. O. Rye, "Isotopes of Sulfur and Carbon," in *Geochemistry of Hydrothermal Deposits*, Ed. by H. Barnes (Wileys, London, 1979), pp. 509–567.
35. E. M. Spiridonov, P. A. Pletnev, E. V. Perelygina, and M. S. Rapoport, *Geology and Mineralogy of the Zolo-*

taya Gora Cupriferous Gold Deposit (Karabash, Middle Urals) (Mosk. Gos. Univ., Moscow, 1997) [in Russian].

36. G. Faure, *Isotope Geology* (Wiley, New York, 1986; Mir, Moscow, 1989).
37. A. V. Ukhanov, V. I. Ustinov, and A. L. Devirts, "Oxygen and Hydrogen Isotopic Compositions of Ultramafic Rocks at the Antigorite Stage of Serpentinization: A Case of Voikarite from the Polar Urals," Geokhimiya, No. 12, 1306–1313 (2002) [Geochem. Int. **40**, 1179–1186 (2002)].
38. S. M. Zhmodik, A. G.Mironov, V. G. Derevenets, et al., "A New Type of Tin–(Mercury)–Gold–PGE Ore Mineralization in the Eastern Sayan Range," Dokl. Akad. Nauk **361**, 510–513 (1998) [Dokl. Earth Sci. **361**, 782–785 (1998)].
39. B. B. Damdinov, S. M. Zhmodik, A. G. Mironov, and Yu. Ch. Ochirov, "Noble-Metal Mineralization in the Rodingites of the Southeastern Part of the Eastern Sayan," Geol. Geofiz. **45**, 577–587 (2004).
40. R. G. Coleman, "Serpentinites, Rodingites and Tectonic Inclusions in Alpine-Type Mountain Chains," Spec. Pap., No. 73 (1963).
41. A. P. Sekerin, "Petrology of Rodingites from the Sayan–Baikal Mountain Area," Dokl. Akad. Nauk SSSR **262**, 175–177 (1982).
42. R. O. Berzon, *Gold-Bearing Ultrabasic Rocks* (VIEMS, Moscow, 1983) [in Russian].
43. D. S. O'Hanley, E. S. Schandl, and F. J. Wicks, "The Origin of Rodingites from Cassiar, British Columbia, and Their Use to Estimate T and $P_{(H_2O)}$ During Serpentinization," Geochim. Cosmochim. Acta **56**, 97–108 (1992).